Studying Polymer-Dispersed Liquid-Crystal Formation by FTIR Spectroscopy. 1. Monitoring Curing Reactions

Rohit Bhargava, Shi-Qing Wang, and Jack L. Koenig*

Department of Macromolecular Science, Case Western Reserve University, Cleveland, Ohio 44106

Received May 4, 1999; Revised Manuscript Received September 27, 1999

ABSTRACT: UV-induced matrix cross-linking is the method of choice to form polymer-dispersed liquid crystals (PDLCs). In this paper, real-time FTIR spectroscopy is applied to study the curing of a model system—a thiolene-chemistry-based prepolymer (NOA65) and its mixtures with liquid crystals. Curing reactions of NOA65 were examined as a function of the film thickness, temperature, and liquid-crystal content. While there was little dependence of the curing behavior on the thickness of the film, the effect of temperature was strong. Curing rates exhibit a maximum around 325 K, while conversions reach a plateau about 20 K higher. The effect of liquid-crystal addition reveals a depression in the conversion. However, compared to the neat matrix, the final conversion was found to be significantly lower only for phase-separating concentrations. The rate of reaction decreased, and the induction period for the onset of polymerizing reactions increased with increasing liquid-crystal concentration. Real-time FTIR spectroscopy is shown to be a viable tool to monitor PDLC formation to optimize curing conditions and characterize the chemical state of components. This provides a basis to allow the morphological structure to be related to observed properties of the film.

Introduction

Polymer-dispersed liquid crystals (PDLCs) are composites containing low molecular weight liquid-crystal domains randomly dispersed in a polymeric matrix.[1] Thin (5−25 μm) films between conducting substrates are used as light shutters whose transmission can be controlled by the application of an electric potential across the film. An empty cell consisting of the substrates as walls is filled with a homogeneous mixture in which phase separation is induced to form PDLCs in situ. Phase separation induced in a homogeneous mixture of prepolymer and liquid crystals by UV-induced matrix polymerization is the current method of choice to produce PDLCs. Photoinduced curing kinetics, phase separation, and nematic ordering are a series of interdependent formation events that have a controlling influence on the properties of the final product. New methods based on photoinduced phase separation that reduce mutual solubility have been suggested,[2] but even they require an investigation of the interplay between reaction kinetics and dissolved liquid crystal.

As a first goal toward an experimental understanding of PDLC formation, it is necessary to observe the reaction kinetics of the curing matrix. Effects of experimental conditions on the photoinduced polymerization kinetics determine the ultimate stability of the film, mutual solubility of the added components, morphology,[3] and electrooptical performance[4] of PDLC films.[5−7] Thus, a study of this aspect of PDLC formation is of academic and commercial importance. Before a prepolymer/liquid-crystal mixture can be cured to give a PDLC, its phase diagram must be determined to know if a chosen curing temperature is in the one-phase or two-phase region. Light scattering, polarized microscopy, and DSC[8−10] have been used to obtain phase diagrams for uncured prepolymer/liquid-crystal mixtures. The curing kinetics of these mixtures have then been examined using photo-DSC by adjusting the temperature to be in the one-phase region[10] and/or the two-phase region.[9] DSC has also been used to examine the curing kinetics of some other polymer/nematic liquid-crystal systems.[11,12]

There is a noticeable absence of systematic studies of matrix curing reactions during PDLC formation by using FTIR spectroscopy. FTIR spectroscopy is an easily accessible, direct, and noninvasive method of examining chemical changes in PDLC films. Real-time FTIR spectroscopy has been used to examine the reaction kinetics of UV-curable systems.[13] Thus, it is a potentially excellent method of conducting a systematic study of a fast curing system like NOA65 considered here. FTIR has the advantage of monitoring specific functional groups almost instantly as opposed to a DSC where a delay in non-chemical-species-specific curing information is expected due to finite time required for heat conduction through the pans, especially in the initial stages of the reaction.[14]

Moreover, as opposed to photo-DSC, FTIR spectroscopy does not require knowledge of heats of reaction for complete conversion, and unlike DSC, there is no deviation involved if reaction enthalpy is a function of conversion. DSC-based methods involve assumptions about the heat released to calculate the extent of reaction, which is expressed as an overall conversion based on heat released for a specific functional group. These drawbacks can be eliminated using real-time FTIR spectroscopy to monitor the formation of such composites. It is the aim of this paper to examine the curing kinetics of the neat matrix as a base case to compare with the kinetics of PDLC precursors. The kinetics are also a useful benchmark to analyze other formation processes.[15]

Prepolymers based on acrylate chemistry have been used as matrix precursors for PDLCs. These materials are easy to handle, mix with liquid crystals at room or elevated temperatures, and cure fast to gelation upon exposure to UV. However, their curing is inhibited by the presence of oxygen (not a major issue when working

* Author to whom correspondence should be addressed.

10.1021/ma990707+ CCC: $18.00
Published on Web 12/03/1999

between substrates), and ever-tightening environmental restrictions may make them suspect for future applications. While retaining most of the advantages, thiolene chemistry based systems do not have such drawbacks. This has led to a renewed interest in such systems[16] after much activity until around 20 years ago.[17] Thiolene-based systems are used as optical adhesives,[18] conformal coatings, and optical fiber coatings. They are also attractive for PDLC systems as they have suitable optical properties to serve as matrices. To go with other advantages, this chemistry apparently has a very high tolerance for stoichiometric imbalances in its development of mechanical properties and, inter alia, of permeability and stability as a matrix for PDLCs. A thiolene-chemistry-based commercial optical adhesive, NOA65, has been used as a model matrix material in a number of studies. Using approximations about the heats of conversion, the "extent of cure" has been determined for the neat matrix and one or two concentrations of liquid crystals using photo-DSC.[8,9] However, reactions of specific functional groups have not been observed. Similarly, the only indication of phase separation during curing comes from detection of strong scattering or onset of turbidity. We use the NOA65-E7 system as a model system to demonstrate the utility of FTIR spectroscopy in monitoring aspects of PDLC formation under given experimental conditions in one single experiment.

Experimental Section

Materials. The low molecular weight liquid crystal used in this study is a liquid-crystal mixture, E7.[19] The nematic–isotropic transition temperature of this system is reported to be about 330 K, with a glass transition temperature of about 210 K. The polymeric matrix, NOA65,[18] is reportedly a UV-curable prepolymer mixture composed primarily of trimethylolpropane diallyl ether, trimethylolpropane tris(thiol), isophorone diisocyanate ester, and a benzophenone photoinitiator.[9] All materials were used as received. A second confirmatory set of experiments was done with a different batch of materials obtained from the same sources.

Sample Preparation. Mixtures by weight of LC and NOA65 were used to prepare the samples. The mixture was weighed, hand mixed for 2 min, and heated to 70 °C (well above the clearing point of E7) for 2 min and mixed again. Samples were cast directly onto a NaCl salt plate containing 10 μm diameter spacers on the edges and sandwiched by another salt plate. The sandwiched assembly was subjected to a constant weight for 15 min to apply pressure in order for it to attain hydrodynamic equilibrium. Constant spacing between the substrates was assured by sandwiching the salt plates between two metal apertures fixed in round brass plates. This assembly is screwed down together and inserted into a heating jacket that also serves as a sample holder. Metal apertures on either side of the salt plate were used for three reasons. They allow the region probed by the IR beam to be away from the boundary (where the spacers were used) and thus free of any boundary effects or influences due to the presence of spacers. The small apertured region was examined before curing using an Olympus Stereo microscope with a 15× magnification to ensure that there were no air bubbles or spacers present in the regions examined. Aperturing also allows the examined material to be surrounded by uncured low viscous material in two dimensions, thus relieving contraction-induced stress.[20] Sample thickness was kept constant with a variation of less than 5% from sample to sample. The mounted sample was subjected to UV radiation at a wavelength of 365 nm obtained using a hand-held UV lamp[21] incorporated into the spectrometer at a fixed position. Thus, the intensity of the UV radiation was held constant for all experiments. Measured intensity of incident UV radiation at the surface of the sample was 1 mW/cm^2 measured using a

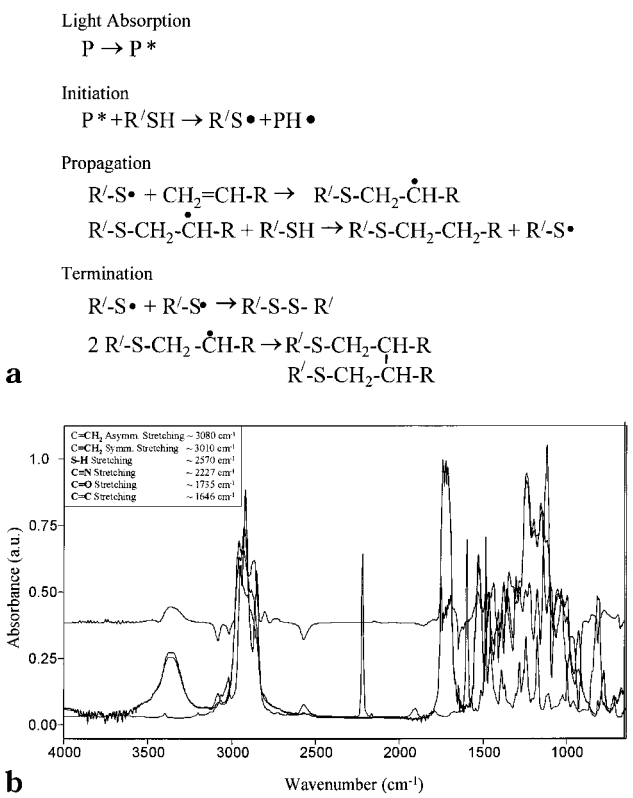

Figure 1. (a) Kinetic scheme for the curing of a thiolene system. (b) Infrared spectra of E7, uncured NOA65, and cured NOA65 and their difference spectrum magnified by a factor of 3. Frequencies in the inset are for the vibrational modes of the bonds indicated in bold.

Series 9811 Radiometer[22] whose least count was 0.01 mW/cm^2. The lamp was allowed to equilibrate for at least a half hour before any experiments were conducted. Temperature was controlled in the custom-built sample holder by using an Omega CN 5000[23] proportional temperature controller. The temperature was also independently measured at a point diametrically across from the measurement for the controller using an Omega HH21 thermocouple based thermometer. Maximum fluctuation in temperature decreased from about ±0.8 K at 300 K to about ±0.2 K at 335 K.

Instrumentation. The FTIR spectrometer used in this study was a Bio-Rad FTS 6000 incorporating an MCT detector.[24] A nominal spectral resolution of 4 cm^{-1} over the mid-infrared range and a time resolution of 0.935 s were used for kinetic studies. This time resolution was deemed sufficiently small to capture the essence of the curing reaction while allowing satisfactorily high signal-to-noise ratio spectra. Five scans were co-added for each data point. Spectral processing was carried out by using the Win-IR Pro v. 2.5 kinetics module[24] and GRAMS 32.

Results and Discussion

Curing Studies of the Neat Matrix-Band Selection. Examining the reaction mechanism detailed in Figure 1a, we see that a number of chemical species may be used to monitor the propagation reaction. These are among the species whose characteristic vibrational bands are identified in Figure 1b along with the mid-infrared spectra for E7, neat uncured NOA65, and neat cured NOA65 and their difference spectrum. The infrared spectrum of uncured sample is obtained and used as a reference, and the difference spectrum is observed over time in our experiments. The negative peaks in the difference spectrum arise from a decrease in the absorbance of reactant species, while the positive ones are

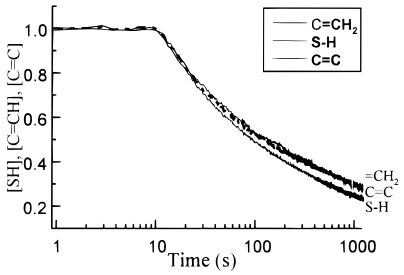

Figure 2. Concentration profiles for different functional groups in a neat NOA65 sample cured at 300 K.

from species formed during reaction. The absorbance of each peak position in the difference spectrum is monitored over time and the absorbance of the uncured precursor is added to it. The time profile of absorbance is then divided by its values at the start of the reaction to normalize the absorbance profile to between 0 and 1.

Normalized profiles of some characteristic bands during curing are shown in Figure 2. The concentration profiles are typical of cross-linking reactions. There is a short induction period, followed by rapid consumption of the monomer and, finally, a much smaller rate of change after gelation. For the neat matrix, the reaction is rapid, and the gel point (as analyzed later in the paper) is reached within 2 min. We monitor the reaction for 20 min, which is about 10 times the time interval to the gel point. We refer to quantities at this point to be in the "final" state as the change past 20 min was not appreciable for any experimental condition examined. Kinetic data from the two reacting species about the conversion trend for the reaction are in good agreement. The symmetric stretching frequency data reveal the same information as that of the asymmetric stretching frequency for the C═CH_2 group. However, its intensity is weaker, and it lies on the left lobe of the aliphatic CH absorbance peaks. Hence, the data are noisier due to the weaker intensity and changing baselines due to the shoulder. Information from the carbon double bond stretching peak (∼1646 cm^{-1}) is similarly obscured as it appears as a shoulder on the carbonyl stretching peak and baselines may be distorted by the presence of water as shown in the spectra. While the difference spectrum alleviates this problem to an extent, an inconsistent instrument purge may produce noise due to a changing vicinity of the peak, which makes the baseline determination error-prone. As a result, while the information agrees very well with that from the C═CH_2 asymmetric stretching peak, deviations around the mean value are much greater. Water vapor subtraction is not a viable technique considering the large number of spectra (1283) in one data set. Moreover, the C═C stretching band itself appears as a band with a shoulder. This is due to the vibrations due to the cis and gauche conformations of the allylic group absorbing at very close frequencies. While the area may be used to calculate conversion (as we have), the band involves a lot of ambiguity. Thus, the C═CH_2 asymmetric stretching vibration peak and the thiol stretching vibration can be used as viable peaks to examine the curing kinetics of this thiolene system.

Aliphatic CH_3, CH_2, and CH stretching modes are highly overlapped, and their appearance can be seen in the difference spectrum. The band positions are complicated by the presence of sulfur and oxygen in the molecules. We did not find any characteristic absorbance of the diisocyanate that is reportedly present in the

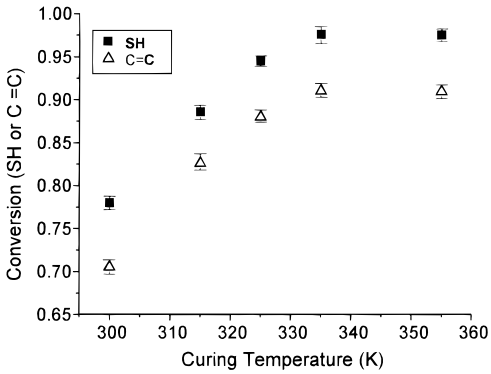

Figure 3. Variation with temperature of conversion at 20 min for two reacting functional groups for neat NOA65.

mixture. There was no evidence of a characteristic strongly absorbing band in the 2300−2250 cm^{-1} region. As the quantity present may be smaller than the detection capability of the instrument, it probably does not affect the thiolene reaction. The presence of an amine could be discerned, and it probably aids in initiating the curing reaction by providing an abstractable α-hydrogen to the activated benzophenone initiator.

Curing Kinetics of the Neat Matrix. The first step in understanding the kinetics of the composite is to examine the curing kinetics of the neat matrix. The effects of UV intensity on photoinduced curing kinetics are well-known[25] and, in general, hold for NOA65. We examine two variables here that may have a large impact on the curing and solubility issues: the thickness of the film undergoing curing and the temperature of the cure. Film thickness has often been the least controlled parameter of photocured PDLCs in the literature. We examined films over a range of thicknesses to observe the effects of changing film thickness and quantify the error introduced by an inadvertent change in thickness, if any. The conversion for two reacting species decreases only a very small extent with increasing cell thickness. The trend is a rather small decrease for each of the curing species and is within the error in measurement. By monitoring the rate of reaction as a function of time, we observed some small differences. However, they are not significant over the 400% change in thickness examined. It may be concluded that a change due to an inadvertent small change in cell thickness during sample preparation introduces a very small error (within experimental error) for quantities of interest.

Even though this variable has no great effect on the curing behavior for our experimental setup, the cell thickness was maintained at 10 μm for all samples. This is the thickness that can be used to maximize signal-to-noise ratios while allowing the nitrile stretching absorption band of the liquid crystal to be observed in its linear absorbance range for all our samples examined. Infrared spectroscopy presents a fast and convenient method of determining the thickness of a film, and prior to all experiments reported in this paper, the film thickness was checked for consistency.

Effect of Temperature on Curing of Neat Matrix. Curing temperature variation introduces an interesting change in the final conversions. The conversion increases with increasing temperature until about 335 K, and is then approximately the same at the next higher temperature examined (Figure 3). This behavior has

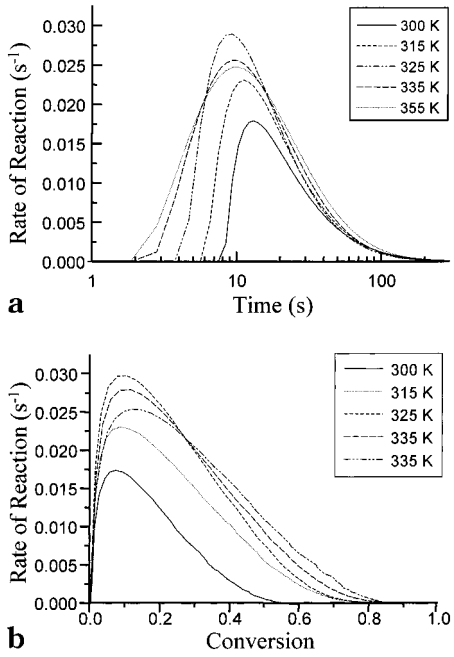

Figure 4. (a) Rate of reaction obtained as a function of time using the rate of change of conversion for neat NOA65 at various temperatures. (b) Rate of reaction as given by the rate of change of conversion for neat NOA65 as a function of conversion for various temperatures.

been seen before, but the maximum conversion was reportedly obtained at higher temperatures.[26] The difference is probably due to differences in incident UV intensity. For our experimental conditions, the extent of cure is close to a maximum at 335 K. This trend is supported by the reported T_gs for the cured neat matrix.[26] NOA65 was reported to achieve a plateau in T_g (approximately 295 K) for curing temperatures higher than about 340 K. This is a direct consequence of the leveling off of the conversion for the two reacting species as seen in Figure 3. A further increase in temperature would not yield appreciably higher conversion, and a temperature overshoot may actually lead to degradation. Thus, studies reported further were conducted at or below this temperature. The results from the double bond specific absorbance data are similar in trend to the thiol group, but the final conversion is lower in all cases. This may be due to the termination reactions by combination involving the radical from the thiol moiety. Error bars are not reported for any data point in which the error is smaller than the range covered due to the size of the symbol.

The rate of reaction at various temperatures is shown in Figure 4a. A striking observation is the decrease in the maximum rate after an increase for the first three observations (also see Figure 4b). The maximum rate of reaction increases until 325 K and then decreases. This observation is consistent with a decrease followed by increase of the cure time constant.[26] The slope of the curves for rate of reaction until the maximum is reached also appear to be different in the two temperature regimes. The rate at which the rate maximum is reached appears to be the same until 325 K and then undergoes a decrease. This points to an increased rate of termination for the propagating radicals above 325 K. Thus, even though radicals may be generated earlier (and possibly, faster), the rate does not reach a maximum until much later due to a decreased lifetime of propagating radicals. It must also be pointed out that

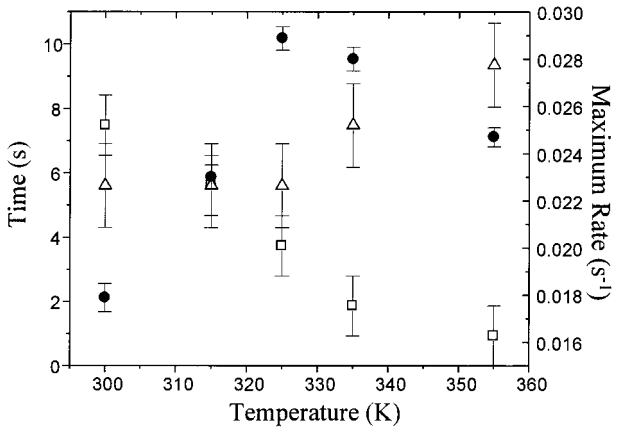

Figure 5. Maximum rate of change of conversion (●), induction time (□), and time difference between maximum rate of reaction and the induction time (▲).

the maximum in rates is lower at higher temperatures, but the total area under the curve (conversion) is larger leading to the trends seen in Figure 3. These trends are consistent with those reported for NOA65[26] and other thiolene[27] systems. The rate maximum was reported to be around 330 K for NOA65, while the maximum in the degree of cure (monitored as a heat released by DSC) was reported to be at about 50 K higher. The rate maximum is seen to be around the same temperature in our case. However, the conversion is close to 100% even at 335 K, and the maxima in conversion probably lie somewhere between 335 and 355 K. Considering the very high values of conversion above 335 K, the point that a higher conversion may lie at higher temperatures is only academic. For all practical purposes, no improvement is achieved in terms of conversion by increasing the temperature beyond 335 K.

The noticeable decrease in induction time is apparent from the starting points of the curves with increasing temperature. Induction time decreases with increasing temperature (Figure 5). The effective time of inhibition is probably dominated by activation energy for the endothermic reaction. The maximum rate occurs at progressively shorter times until 325 K. Temperatures higher than 325 K take a longer time interval to reach the maximum despite shorter induction times. The time period between the onset of reaction and the occurrence of the maximum rate is approximately the same for the first three temperatures but increases for the next two. This again implies that the initiation and initial polymerization are probably different for the two highest temperatures. The same trends can be seen if the rate of reaction is plotted against conversion (Figure 4b). The maximum rate of reaction is reached at approximately the same conversion for the first three temperatures. This seems to suggest that the initial generation of radicals and reaction is not dependent on the temperature. It also appears that the viscosity difference introduced by the higher temperatures has only a marginal effect. This is to be expected for the low viscosity oligomers. The increased region along with an increased slope for the post-maximum rate regime increases with increase in temperature until 325 K. That trend is a direct consequence of the increased mobility due to higher temperatures. Dilution would lead to the same broadening in this type of plot without the increased rates. That result can be expected for PDLC mixtures and is seen later in the paper. Fitted curves to the derivative time profiles of the normalized

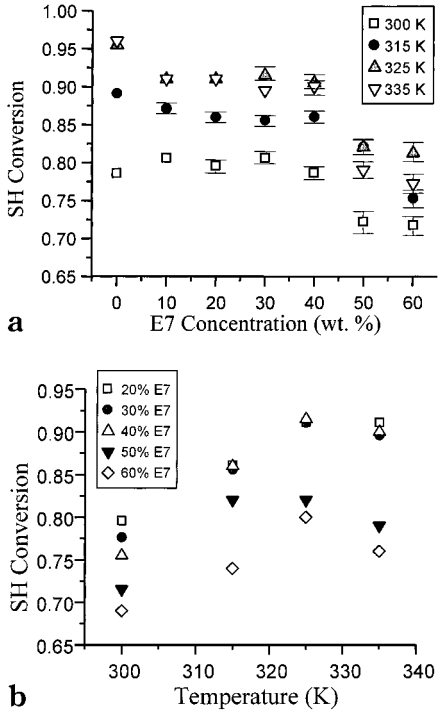

Figure 6. (a) Final thiol conversion as a function of liquid-crystal content at different temperatures. (b) Final thiol conversion for different concentrations of liquid crystal in the initially homogeneous mixture as a function of temperature.

conversion are shown, as the error in the later stages of the reaction tends to obscure the trends of the curves. The typical error itself can be seen as error bars on the rate values in Figure 5. The temperatures examined above are below the temperature for commencement of thermally induced polymerization reactions. This was also evident in absorbance spectra (not shown in the paper) that are identical for samples prepared at 300 K and those heated to 365 K and brought back to 300 K.

Curing of the Matrix in Precursor−Liquid-Crystal Mixtures. Now that the curing of the neat matrix has been analyzed as a base case, we can examine the curing kinetics for initially homogeneous mixtures of NOA65 with E7. The phase diagram of the E7/NOA65 has previously been reported.[8] Limiting our studies to the one-phase region from those plots, certain concentrations are not examined at lower temperatures. The conversion of the thiol group for initial mixtures as a function of curing temperature can be seen in Figure 6a. The C═CH stretching vibration was overlapped by other CH vibrations in the system and, hence, could not be used for monitoring the cure.

At 300 K, the final conversion of low liquid-crystal-concentration mixtures is actually marginally higher than that of the neat matrix in some cases. This can be attributed to the decrease in viscosity by the addition of a small amount of diluent. In all cases, addition of liquid crystal shows a small decreasing trend or plateau in the initial concentrations and exhibits a decrease and downward trend for higher concentrations. The final conversion for a 50% E7 matrix is close to about 90% that of the pure matrix. This is in excellent agreement with reported values.[26] Comparing the concentrations where the final conversion falls off with the minimum concentration that phase separates at each temperature,[15] it can be seen that the two transition concentrations correspond well. It has been suggested that a reduced final conversion for phase-separating systems could be due to the preferential dissolution of the initiator in the phase-separating liquid crystal. However, the same trend would also be possible if the matrix material dissolved in the liquid-crystal domains was unreacted. A larger fraction of added NOA would be soluble in a larger phase-separated fraction of the liquid crystal, and thus, the final conversion would be expected to decrease with E7 concentration. This decrease would also not be linear as the phase separation would not begin at the same point of time/cure state of the matrix. A sharper than linear drop is to be expected, and that is seen in our case. A similar argument would hold for preferential photoinitiator dissolution in the LC domains, which would result in the matrix being cured to a smaller degree. However, the drop that is seen in conversion for phase-separated samples at these very long times can probably only come about if the matrix material in the droplet were uncured. Excess photoinitiator in the droplets would mean that the trend in decrease of conversion would continue on a smooth curve with the matrix conversion decrease being offset by the increase in conversion of the material in the droplets. Hence, the likely situation is that the matrix material is at a much lower conversion inside the droplets. This has important implications for property development and the electrical response of the nematic domains.

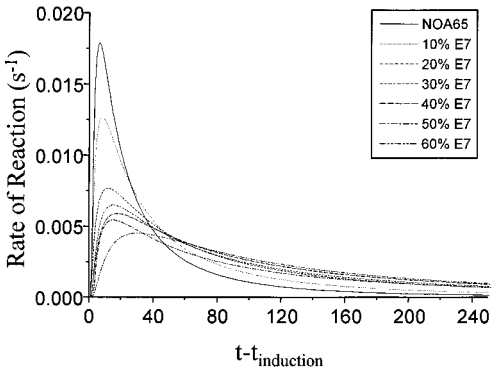

Figure 7. Rate of reaction as given by the rate of change of conversion for Initially homogeneous NOA65/E7 mixtures at 300 K.

If the variation with temperature is examined along a single concentration, the conversion is seen to reach a plateau for smaller concentrations while the larger liquid-crystal-concentration mixtures show a maximum in the conversion. Trends for a few concentrations are shown in Figure 8b. The values are essentially the same for samples with liquid-crystal content below 40%, and a variation of the higher concentrations can be seen to go through maxima in conversion. The rate of conversion of the thiol group is monitored as a function of E7 concentration and the data is shown in Figure 7 as a rate of change in normalized absorbance. The maximum rate of reaction decreases with the addition of liquid crystal. Even a small amount of liquid crystal decreases the rate appreciably. The maximum reaction rate as a function of concentration can be seen in Figure 8a. The rate decreases with addition of liquid crystal for all temperatures but increases with temperature. At the same time, the induction time increases with the addition of liquid crystal (Figure 8b) but decreases with temperature.

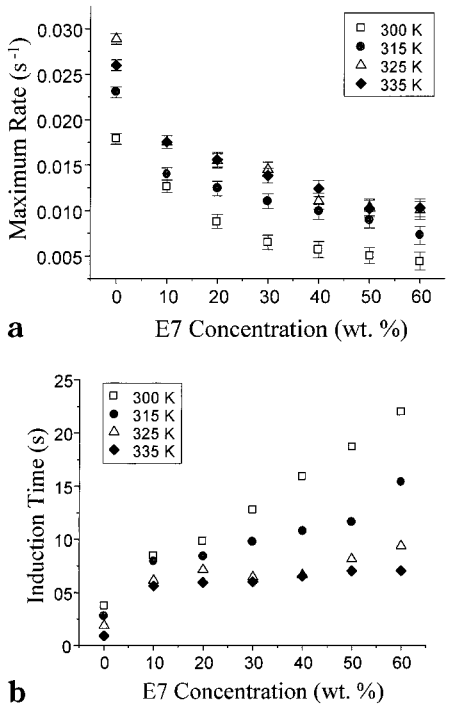

Figure 8. (a) Maximum rate of reaction as a function of E7 concentration for different temperatures. (b) Induction time as a function of E7 concentration for different temperatures.

The reaction rate is typical of such cross-linking reactions. In general, the curing kinetics of multifunctional materials exhibit a variety of interesting and complicating features:[28] autoacceleration, autodeceleration, unequal functional group reactivity, diffusion limited reactivity, formation of local "microgels", and a delay in volume shrinkage. The autoacceleration and -deceleration are primarily dependent on initiator concentration, incident UV intensity, and temperature. The first two being held constant in our study, the rate of reactions at different temperatures can be seen in Figure 4b. Acceleration is brought about by the production of a large number of reactive radicals in a low viscosity prepolymer at the start of the reaction. The number of radicals produced per unit volume decreases with the addition of liquid crystal, and hence, the maximum rates achieved are expected to be lower. This rate lowering is partly aided by the absorption of UV radiation by the conjugate aromatic systems in the liquid crystal and is opposed by the decrease in viscosity of the matrix due to dilution. The dilution effect is not expected to be important in the initial stages as the prepolymer has a very low viscosity itself, but it affects the later stages of polymerization. The effect results in a lower initiation rate manifested as a smaller slope with increasing LC concentration for rate plots in Figure 7.

The fast rate of reaction quickly results in a maximum of the rate being attained followed by a period of deceleration. The deceleration process is brought about by a decrease in reactive species and a loss in mobility of radicals due to increased matrix viscosity and incorporation of the radicals into growing chains. Addition of liquid crystals serves to plasticize the matrix, and thus, deceleration is not as sharp as for the neat matrix. Reaction rates are still appreciable for higher liquid-crystal contents even after the neat matrix has reached very low rates approaching gelation. This trend can be seen in the later times of the rate plots (Figure 7), where the rate of reaction for the liquid-crystal-rich mixtures is greater than that for initially LC-poor mixtures.

Gelation results in a rate drop of orders of magnitude as reaction rates are dominated by slow diffusion of radical through a high viscosity medium. If the rate of reaction is plotted as a function of conversion for the neat matrix (Figure 4b), these features can clearly be seen and the conversion at gelation determined. It has been proposed that the conversion for gelation is essentially independent of temperature.[29] We see an increase in the conversion at gelation with increasing temperature for our system. The effect of increasing temperature is to increase the rate of cross-linking, and hence the time required to attain gelation also decreases. Phase separation tends to obscure features in the later stages as different curing reactions progress in a variety of liquid-crystal concentrations. Liquid-crystal addition also alters the rate of reaction by absorbing some UV radiation. The effect is probably more pronounced for the relatively moderate intensity used by us. Phase separation would result in additional UV intensity losses due to scattering. These are other complicating factors in the reaction conditions and kinetic behavior during PDLC formation.

An induction time before the start of polymerizing reactions can be seen as the initial plateau in the time profile of the normalized absorbance of peaks attributed to reacting species (see Figure 2). This is due to the presence of inhibitors that combine with the initiator or propagating radical to convert them to nonreactive species or species with reactivity lower than what is required for polymerization.[25] Oxygen also acts as an effective inhibitor for the initiation step but not for the propagating step in thiolene systems. Since our system is closed, only dissolved oxygen would have an impact. The addition of liquid crystal serves to increase the induction time. It is probably the consequence of dissolved air or impurities present in E7. The decrease in induction time with an increase in temperature has also been noted in other UV-curable systems.[30] As the liquid-crystal concentration increases or the temperature decreases, the induction time decreases. The time taken to reach the maximum curing rate shows a similar trend in another system.[12] The sharp onset of polymerizing reactions after this time is indicative of the effectiveness of this inhibitor. The reaction kinetics are expected to follow the uninhibited kinetics by a time lag after the inhibitor is consumed.[25] Hence, its effect on the kinetics can be eliminated by using the induction time as a reference instead of the time when the UV lamp was turned on.

We were not able to reliably observe any spectroscopic changes in this initial time period, probably due to the very low concentration of the inhibitor. The induction time from DSC measurements should be larger compared to FTIR spectra by a (speculated) few seconds[31] to less than half a second.[32] We did not find any reported values for the induction time in DSC studies for this system in the literature. A real-time FTIR study of UV-induced curing in a thiolene system[13] did not report an induction time either. This was probably because they used a time resolution of 10 s, which is too large to pick up the induction time if values obtained in this paper are typical of neat thiolene systems.

A single UV intensity and a limited temperature range were examined in this study. The effect of changing UV intensity is well-known.[12,25,26] Similar

trends may be expected for the system discussed here. The effects of UV intensity on the liquid-crystal phase separation and phase behavior are very small[26] and are, thus, relatively unimportant for the solubility studies section reported in this paper. We have reported observations of the curing reactions of the matrix without any kinetic analysis. The curing kinetics of a thiolene system has been analyzed in some detail elsewhere.[13] The kinetic analysis of the curing of NOA65 is similar. The curing kinetics of mixtures in the two-phase region were not examined as they are complicated by the dynamics of phase separation and require a more detailed analysis. However, the techniques described in the paper may well be applied to those cases too. Phase separation may result in different curing kinetics for different spatial regions of the sample and would thus, depend on the size of the domain, its organization state and boundary layer profile. Scattering and optical effects may also complicate UV intensity distribution. Phase separating mixtures also require simultaneous solution of chemical potential balance equations for each phase. Those aspects are dealt with in a separate publication,[33] as our aim here was only to demonstrate the ability of real-time FTIR to acquire chemical information and report the various features of such reactions from which kinetic information, reaction pathways and morphology development signals may be derived. Only the final values and the uninterrupted process of formation were examined in the study. The issue of how the morphology of these systems is affected by their curing temperature and liquid-crystal concentration has been partially examined.[34] Further studies are in progress that would aim to relate the curing behavior seen here to the developed morphology.

Conclusions

The UV-induced curing kinetics of a widely used, thiolene-chemistry-based adhesive, NOA65, have been analyzed using real-time FTIR spectroscopy. The curing kinetics were not affected by cell thickness. In general, increasing the temperature of curing results in an increase in the final conversion and rate of conversion. The rate of reaction reached a maximum at 325 K, while conversion attained the plateau at 335 K. Addition of liquid crystal results in a depression of the rate of reaction and final conversions. However, the final conversion is significantly lower only for phase-separating compositions. Coupled with other evidence, it is proposed that the dissolved matrix material in the nematic domains is cured to a smaller extent than the matrix. As the fraction of nematic domains increased, the final conversion obtained decreased. An increase in temperature of curing resulted in higher rates and conversions for a given concentration. The plateau in reaction rate and conversion was shifted to lower temperatures by addition of liquid crystal. These trends would help quantify the formation process and determine the chemical state of the matrix achievable under given experimental conditions. Real-time FTIR spectroscopy is applied to examine the curing kinetics of PDLC formation and is suggested as a convenient tool to optimize the formation of PDLCs under given conditions.

Acknowledgment. Funding for the project was provided by the National Science Foundation Center for Advanced Liquid Crystalline Optical Materials (ALCOM).

References and Notes

(1) Doane, J. W. In *Liquid Crystals-Applications and Uses*; Bahadur, B., Ed.; World Scientific Publishing: Singapore, 1990; Vol. 1, p 361.
(2) Bhargava, R.; Wang, S.-Q.; Koenig, J. L. *Macromolecules* **1999**, *32*, 2748.
(3) Lovinger, A. J.; Amundson, K. R.; Davis D. D. *Chem. Mater.* **1994**, *6*, 1726.
(4) Nazarenko, V. G.; Sarala, S.; Madhusudana, N. V. *Jpn. J. Appl. Phys 1.* **1994**, *5A*, 2641.
(5) Yamagishi, F. G.; Miller, L. J.; van Ast, I. C. *Liquid Crystals Chemistry, Physics and Applications*; Proccedings of SPIE-The International Society for Optical Engineering No. 1080; SPIE: Bellingham, WA, 1989; p 24.
(6) Legrange, J. D.; Carter, S. A.; Fuentes, M.; Boo, J.; Freeny, A. E.; Cleveland, W.; Miller, T. M. *J. Appl. Phys.* **1997**, *81*, 5984.
(7) Carter, S. A.; Legrange, J. D.; White, W.; Boo, J.; Wiltzius, P. *J. Appl. Phys.* **1997**, *81*, 5992.
(8) Smith, G. W. *Phys. Rev. Lett.* **1993**, *70*, 198.
(9) Nwabunma, D.; Kim, K. J.; Lin, Y.; Chien, L. C.; Kyu, T. *Macromolecules* **1998**, *31*, 6806.
(10) Smith, G. W. *Mol. Cryst. Liq. Cryst.* **1994**, *239*, 63.
(11) Smith, G. W. *Mol. Cryst. Liq. Cryst.* **1994**, *241*, 77.
(12) Roussel, F.; Buisine, J.-M. *Liq. Cryst.* **1998**, *24*, 555.
(13) Chiou, B.-S.; Khan, S. A. *Macromolecules* **1997**, *30*, 7322.
(14) Guymon, C. A.; Bowman, C. N. *Macromolecules* **1997**, *30*, 5271.
(15) See the second part of this series by the authors of this paper. Part 2. Bhargava, R.; Wang, S.-Q.; Koenig, J. L. *Macromolecules* **1999**, *33*, 8989.
(16) Chiou, B.-S.; English, R. J.; Khan, S. A. *Macromolecules* **1996**, *29*, 5368.
(17) Morgan, C. R.; Magnotta, F.; Ketley, A. D. *J. Polym. Sci., Polym. Chem. Ed.* **1977**, *15*, 627.
(18) Norland Products Inc., North Brunswick, NJ.
(19) EM Industries, Inc., 7, Skyline Drive, Hawthorne, NY 10532.
(20) Tran-Cong, Q.; Harada, A. *Phys. Rev. Lett.* **1996**, *76*, 1162.
(21) UVP Inc., San Gabriel, CA 91778.
(22) Cole-Parmer Instrument Company, Chicago, IL 60648.
(23) Omega Engineering Inc., One Omega Drive, Box 4047, Stamford, CT 06907-0047.
(24) Bio-Rad Laboratories, Digilab Division, 237 Putnam Avenue, Cambridge, MA 02139.
(25) Odian, G. *Principles of Polymerization*, 3rd ed.; Wiley-Interscience: New York, 1991; pp 259−267.
(26) Smith G. W. *Mol. Cryst. Liq. Cryst.* **1991**, *196*, 89.
(27) Hoyle, C. E.; Hensel, R. D.; Grubb, M. B. *J. Polym. Sci.* **1984**, *22*, 1865.
(28) Kloosterboer, J. G. *Adv. Polym. Sci.* **1988**, *84*, 1.
(29) Izuka, A. I.; Winter, H. H.; Hashimoto, T. *Macromolecules* **1994**, *27*, 6883.
(30) Cook, W. D. *Polymer* **1992**, *33*, 2152.
(31) Decker, C.; Moussa, K. *Macromolecules* **1989**, *22*, 4455.
(32) Dietz, J. E.; Elliot, B. J.; Peppas, N. A. *Macromolecules* **1995**, *28*, 5163.
(33) Bhargava, R.; Wang, S.-Q.; Koenig, J. L. Manuscript under preparation.
(34) Nephew, J. B.; Nihei, T. C.; Carter, S. A. *Phys. Rev. Lett.* **1998**, *80*, 3276.

MA990707+